

# On the application of hybrid turbulence models for fuel spray simulation in modern internal combustion engines

Cite as: AIP Conference Proceedings 2191, 020095 (2019); <https://doi.org/10.1063/1.5138828>  
Published Online: 17 December 2019

Vesselin K. Krastev, and Giovanni Di Ilio



View Online



Export Citation

## Lock-in Amplifiers up to 600 MHz



Zurich  
Instruments



# On the Application of Hybrid Turbulence Models for Fuel Spray Simulation in Modern Internal Combustion Engines

Vesselin K. Krastev<sup>1,a)</sup> and Giovanni Di Ilio<sup>2</sup>

<sup>1</sup>*Department of Enterprise Engineering “Mario Lucertini”, University of Rome “Tor Vergata”  
Via del Politecnico, 1 - 00133 Rome (Italy).*

<sup>2</sup>*Department of Engineering, University of Rome “Niccolò Cusano”  
Via Don Carlo Gnocchi, 3 - 00166 Rome (Italy).*

<sup>a)</sup>Corresponding author: v.krastev@unitus.it; v.krastev84@gmail.com

**Abstract.** In order to satisfy the increasingly restrictive EU norms on air pollutant emissions, most of the world-leading passenger car manufacturers are currently forced to apply different engine electrification solutions to a large part of their model portfolio, ranging from Mild-Hybrid Electric Vehicles (MEHVs) to Plug-in Hybrid Electric Vehicles (PHEVs). Nonetheless, the efficient design of the thermal engine part still plays a fundamental role in the overall fuel consumption and polluting emissions reduction. Both gasoline-fueled and diesel-fueled modern engines rely on finely tuned direct fuel injection strategies, in order to simultaneously optimize primary energy consumption and particulate matter and/or gaseous emissions. Therefore, it is of foremost importance to develop robust and reliable multidimensional numerical tools, to support engineers during the injection system design and testing processes. In that sense, turbulence modeling is a key point for the accurate description of fuel spray evolution and mixture formation, due to the very high injection pressures (in diesel-fueled engines) or the complex spray patterns and severe flow cyclic variability (in downsized, turbocharged, gasoline-fueled engines). In the present paper, we evaluate the usage of hybrid URANS/LES turbulence modeling techniques for fuel spray simulation, based on the current scientific literature on this topic and on some recent computational studies from the authors. Aspects such as the comparison with URANS and standard LES models are discussed, and strengths and weaknesses of the analyzed hybrid approaches are pointed out. The authors assume that this work could pave the way for further debates on the potential vs. actual benefits of mixing statistically-derived (URANS) and scale-resolving (LES) turbulence modeling options for engine flow simulation.

## INTRODUCTION

As of 2017, the European Commission has introduced new and more reliable emissions tests in real driving conditions (*Real Driving Emissions - RDE*) as well as an improved laboratory test (*World Harmonised Light Vehicle Test Procedure - WLTP*) for light vehicles that are meant for driving on European roads [1]. In conjunction with full Euro 6d compliance approaching in 2020, this is going to drastically cut down NO<sub>x</sub> and particulate matter emissions for both diesel-fueled and gasoline-fueled new car models. As such, the role of high-fidelity Computational Fluid Dynamics (CFD) is becoming prominent for the development of the next-generation direct-injection thermal powertrains.

Several approaches are currently available for the multidimensional description of fuel sprays, such as the Eulerian Spray Atomization (ESA), Volume Of Fluid (VOF) and Eulerian-Lagrangian (EL) methods. As discussed in [2, 3] and references therein, the ESA approach generally works well for the dense part of the spray and at very high Reynolds and Weber numbers, which are typical of some operating conditions in diesel injectors (turbulence-driven atomization process). However, ESA modeling is also computationally expensive, quite sensitive to the turbulence modeling treatment and does not allow to correctly describe the spray velocity field whenever interfacial dynamics becomes dominant (i. e. at low injection pressures and ambient densities). The VOF method has been applied since 2000 for internal and external spray flow computations [4, 5, 6, 7, 8, 9, 10], due to the accurate interface-tracking capability across all the phases involved (up to three in cavitating injectors). However, the extremely high computational cost required for the resolution of the spray breakup process does not allow the VOF integration into complete engine cycle modeling. The current *de-facto* standard for industry-grade multidimensional modeling of direct-injection engines is represented by the EL approach, in which the gaseous phase is treated as a continuum while the liquid

phase is described through a Lagrangian Particle Tracking (LPT) method. As opposed to ESA, the LPT method is well formulated for the diluted spray region while it commonly requires *ad-hoc* parameter tuning for the near-nozzle flow development, including the primary breakup process.

A fundamental aspect of LPT is the way turbulence is accounted for, as it greatly influences the spray particle dynamics and, as such, the spray pattern and fuel mixing in the engine combustion chamber. Typically, the turbulence modeling task is addressed through time-dependent forms of RANS-based turbulence closures, also known as unsteady-RANS (URANS) methods. URANS models are computationally cheap and allow to achieve reasonable overall accuracy levels, but they also introduce further model-specific dependence and are unable to capture the local mixture fraction perturbations due to different sources of cycle-to-cycle variability. A further option for turbulence modeling is represented by Large Eddy Simulation, which is able to accurately reproduce local and instantaneous flow changes through appropriate time and space filtering of the Navier-Stokes equations. As such, LES has been extensively developed for engine modeling in the past 20 years [11], making significant progress towards full industry-grade maturity [12, 13]. In spite of this, LES/LPT coupling is still relatively new [14, 15, 16, 17, 18], thus suggesting the need for further developments in this area. Two of the main issues that are still not completely solved are:

1. *Numerical resolution* - The LES working principle requires a sufficiently small grid and time step size, in order to resolve at least the most energetic flow structures at a specific flow regime. Such requirement usually matches well LPT in the diluted spray region [16], which is characterized by small velocity gradients and small spray droplets. On the other side, the near-nozzle high-speed spray region may require significant mesh refinement levels for LES to accurately describe turbulent phenomena, which in turn may violate some of the hypotheses that lie behind the Lagrangian tracking concept (i. e. small particle size compared to the grid spacing).
2. *Sub-grid turbulent dispersion* - The correct evaluation of the droplet-gas relative velocity requires a modeling assumption for velocity fluctuations at a sub-grid level. One of the most common choice is to adapt stochastic dispersion models originally developed for the RANS framework, which however can easily return unphysical spray particle trajectories in LES/LPT simulations [18]. Although there is still no clear consensus on how to develop LES-oriented sub-grid dispersion models, it is apparent that their impact should not be neglected, especially for what concerns liquid mass fraction distribution at certain spray regimes [17, 18].

A potential remedy for Point 1 is represented by hybrid URANS/LES turbulence models. In principle, URANS/LES hybrids should be able to adapt their behavior by applying the best turbulence modeling option with respect to the available numerical resolution, which is seemingly attractive for EL spray modeling due to the above mentioned resolution issues. Nonetheless, even if the number of engine-related hybrid studies is constantly increasing in the last decade [19, 20, 21, 22, 23, 24, 25, 26, 27, 28, 29, 30, 31, 32, 33], hybrid/LPT investigations are still very scarce in the literature [34, 35, 36, 37]. As such, in the present work we propose a discussion on the applicability of URANS/LES hybrids to EL spray modeling in internal combustion engines, essentially based on our latest findings on this topic. The remaining part of this paper is organized as follows: first, the adopted hybrid turbulence modeling strategy is briefly outlined; after that, results for a reference diesel injector and for a reference GDI injector are analyzed and, finally, conclusions and future perspectives are drawn.

## APPLICATIONS

### Hybrid formulation

The hybrid turbulence modeling used in the present work has already been extensively described in a number of previous publications (see e. g. [35] and references therein), so here only the main aspects will be recalled. The hybrid model is based on a limited time scale *k-g* URANS formulation [38, 39, 40], that is:

$$\rho \frac{\partial k}{\partial t} + \nabla \cdot (\rho \mathbf{U}k) = \mathcal{P} - \mathcal{S}_k + \nabla \cdot \left[ \left( \frac{\mu_t}{\sigma_k} + \mu \right) \nabla k \right] \quad (1)$$

$$\rho \frac{\partial g}{\partial t} + \nabla \cdot (\rho \mathbf{U}g) = \rho \frac{\beta g}{2\beta^* \tau} - \frac{\alpha g^3}{2k\tau} \mathcal{P} + \nabla \cdot \left[ \left( \frac{\mu_t}{\sigma_g} + \mu \right) \nabla g \right] + \left( \frac{\mu_t}{\sigma_g} + \mu \right) \frac{3g}{\tau} (\nabla g \cdot \nabla g) \quad (2)$$

$$\mu_t = \rho \beta^* k \tau \quad (3)$$

with  $\mu_t$  being the dynamic turbulent viscosity,  $\rho$  being the fluid density and  $\alpha, \beta, \beta^*, \sigma_k, \sigma_g$  being model closure constants. The turbulent time scale  $\tau$  is then given by [40, 41, 42]:

$$\tau = \min(g^2, a_\tau \tau_{lim}) \quad (4)$$

$$\tau_{lim} = \frac{2}{3\beta^*} \sqrt{\frac{3}{8|\mathbf{E}|^2}} \quad (5)$$

with  $|\mathbf{E}|^2 =$  magnitude squared of the mean rate-of-strain tensor and  $a_\tau \leq 1$  being a further model constant. According to [42], the recommended value range for  $a_\tau$  is  $0.6 \leq a_\tau \leq 1$ . In the present work  $a_\tau$  is assumed equal to 0.8 [35].

A DES-type hybrid model is easily derived from Equations (1)-(3), by the following sink term modification [43]:

$$\mathcal{S}_{k,RANS} = \rho \frac{k}{\tau} = \rho \frac{k^{3/2}}{l_{RANS}} \quad (6)$$

$$l_{RANS} = k^{1/2} \tau \quad (7)$$

$$\mathcal{S}_{k,DES} = F_{DES} \mathcal{S}_{k,RANS} \quad (8)$$

$$F_{DES} = \max\left(\frac{l_{RANS}}{C_{DES} \Delta}, 1\right) \quad (9)$$

where  $\Delta$  is a spatial filter width, related to the local grid spacing, while  $C_{DES} = 0.5$  [28]. Equation (9) represents a typical *seamless* DES mode of operation [44, 45], in which the turbulent viscosity scaling switches between URANS-type and LES-type depending on the  $l_{RANS}/(C_{DES} \Delta)$  ratio (LES is triggered for  $l_{RANS}/(C_{DES} \Delta) > 1$ ).

To extend its usability, Equation (9) can be rearranged in a zonal form, namely [28]:

$$F_{DES}^* = C_{z1} F_{DES} + (1 - C_{z1}) F_{ZDES} \quad (10)$$

$$F_{ZDES} = C_{z2} + (1 - C_{z2}) \left(\frac{l_{RANS}}{C_{DES} \Delta}\right) \quad (11)$$

where the URANS, DES or LES behavior is fixed *a-priori* by the user in different parts of the computational domain, depending on the combined  $C_{z1}$  and  $C_{z2}$  values (see Table 1). In the present work, only a single Mode at a time has been tested, in order to evaluate which one should return the most reliable predictions into a hypothetical spray-injection/in-cylinder zone.

TABLE 1: Modes of operation of  $F_{DES}^*$ .

$C_{z1}$	$C_{z2}$	Simulation type	Mode
0	1	URANS	I
0	0	LES	II
1	1/0	DES	III

Note that the turbulent transport equations keep the same form whichever the mode of operation, thus guaranteeing continuity of the transported turbulent scalars across different zones of the domain.

## The spray-A case

The ECN non-reacting ‘‘Spray A’’ [46] is selected as a reference diesel injector case for the present paper (see Table 2 for the main spray operating parameters). All the numerical predictions reported here have been obtained within the OpenFOAM-6 open-source CFD framework [47], which has been applied on a box-shaped computational domain of 108 x 108 x 108 mm. The inlet massflow profile used in simulations is generated through the utility purposely developed at the Universitat Politècnica de València for the ‘‘Spray A’’ modeling [48], as shown in Figure 1. For other details on the numerical settings, the reader is redirected to [35]. Here, only the salient features of the computational grids are reported in Table 3 and Figure 2.

TABLE 2: ‘‘Spray A’’ nozzle characteristics and operating conditions.

Fuel type	n-dodecane ( $C_{12}H_{26}$ )
Ambient composition (by volume)	0% $O_2$ 6.52% $CO_2$ 3.77% $H_2O$ 89.71% $N_2$
Ambient gas temperature	900 K
Ambient gas pressure	6.0 MPa
Ambient gas density	22.8 kg/m <sup>3</sup>
Injection duration	1.5 - 6 ms
Injection mass	3.56 - 15.12 mg
Injection pressure	150 MPa
Injection temperature	363 K
Discharge coefficient	0.89
Injector nozzle diameter	90 $\mu$ m

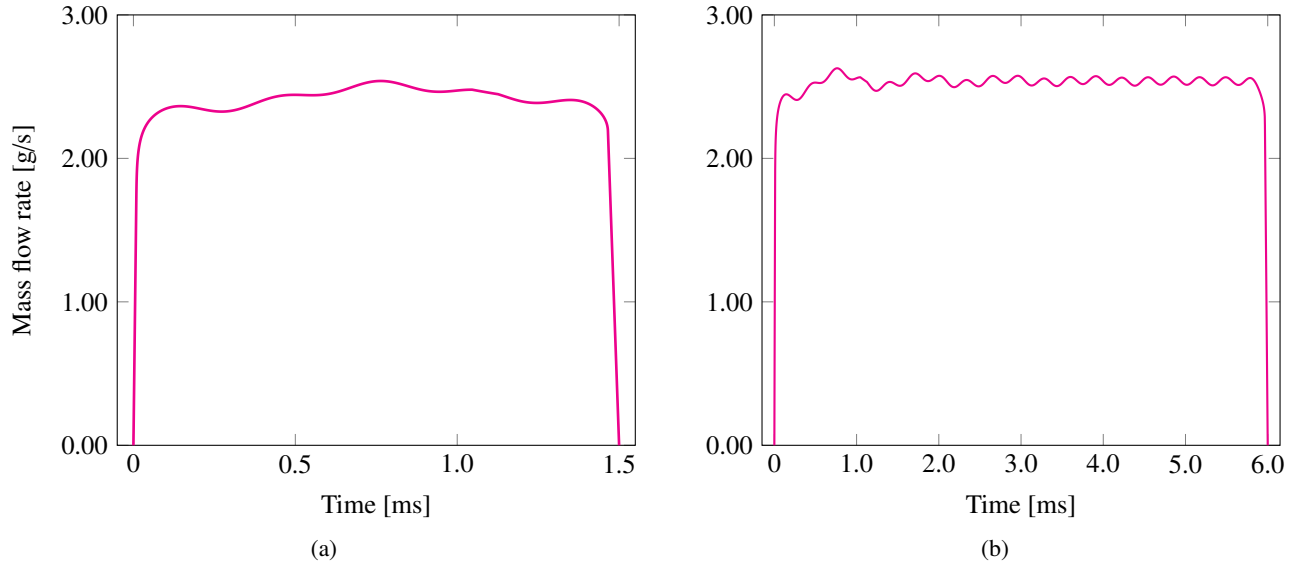


FIGURE 1: Standard ROI profiles used as inflow condition in the ‘‘Spray A’’ simulations: a) 1.5 ms injection; b) 6 ms injection.

TABLE 3: Grid refinement distribution for the Coarse (C), Medium (M) and Fine (F) “Spray A” meshes.

Refinement level	Size [mm]	Radius [mm]			Height [mm]		
		C	M	F	C	M	F
1	2.0000	30	30	30	80	80	80
2	1.0000	15	15	15	70	75	75
3	0.5000	10	10	10	20	70	70
4	0.2500	8	8	8	10	65	65
5	0.1250	7	7	7	5	60	60
6	0.0625	\	\	5	\	\	58

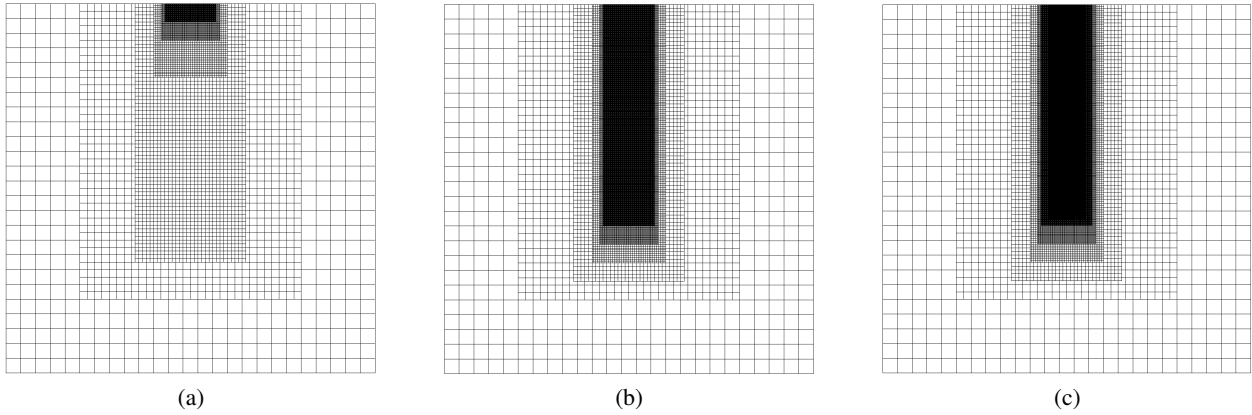


FIGURE 2: Axial section of the “Spray A” meshes; a) Coarse; b) Medium; c) Fine. Figure adapted from [35].

A selection of the results obtained in Modes I and III is shown in Figures 3-5. Predictions from URANS (Mode I) refer to the mesh C, which already guarantees a sufficient numerical convergence level for such turbulence modeling, whereas for DES (Mode III) predictions are obtained with mesh M. Note that the same Lagrangian spray constants are applied in both cases, in order to isolate the effects of turbulence treatment with respect to the breakup modeling parameters [35].

Interestingly, liquid and vapor fuel penetration profiles are very similar among each other, with only a slightly more accurate vapor penetration trend returned by DES (Figure 3). This finding becomes even more interesting if an analysis of the  $1/F_{DES}^*$  function distribution is performed for the Mode III simulation, as shown in Figure 4. From such analysis, it is apparent that the spray remains in URANS state only at the very beginning of injection, then rapidly turning into a LES-type behavior. This suggests that, at the reported “Spray A” conditions, the *seamless* DES formulation operates very close to a pure-LES mode.

Figure 5 shows centerline and radial profiles of the axial velocity component, which mimics the experimental campaign performed at the IFPEN for further “Spray A” characterization [46]. Given also the experimental measurement uncertainty, the DES mode seems to return a more consistent centerline velocity trend, while radial profiles are quite close one to each other and in fairly good agreement with the experiments.

### The spray-G case

The ECN “Spray G” [46] is the GDI reference counterpart of the “Spray A”. The “Spray G” is characterized by an 8-hole injector, with the main injection parameters summarized in Table 4. For the construction of the “Spray G” computational grid, the ratio between the minimum cell size and the injector hole diameter has been kept similar to the “Spray A” M grid, thus leading to an absolute minimum cell size of 0.25 mm (see also Figure 6b). The inlet ROI profile is shown in Figure 6a, while the remaining part of the numerical setup is essentially similar to what already defined for the “Spray A” case.

Figures 7 and 8 show preliminary outcomes for the “Spray G” case, obtained for Mode III of the proposed

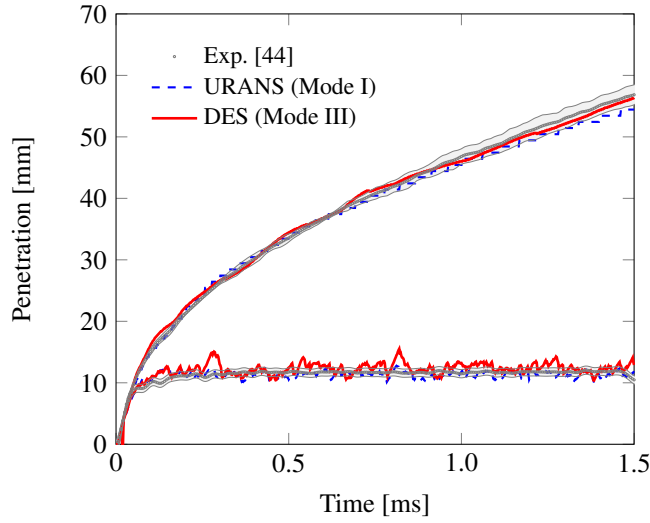


FIGURE 3: Liquid and vapor penetration for the Modes I and III of the  $k$ - $g$  hybrid formulation; Mode I (URANS) results are obtained on mesh C, Mode III (seamless DES) results are obtained from mesh F. The filled area corresponds to the experimental standard deviation.

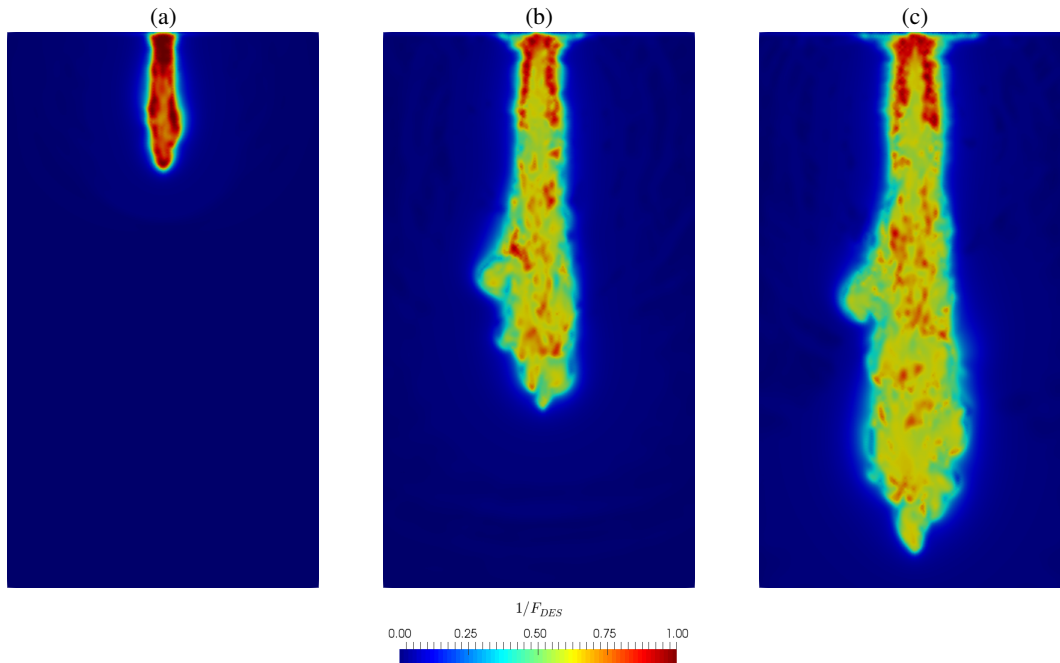


FIGURE 4: Evolution of  $1/F_{DES}^*$  in a Mode III (seamless DES) simulation of the “Spray A” case, at: a)  $t = 0.03$  ms, b)  $t = 0.12$  ms, and c)  $t = 0.21$  ms after SOI. Figure adapted from [35].

hybrid formulation. The spray pattern is consistent with the previous “Spray G” studies, although the breakup and evaporation parameters have yet to be fully established for DES. Notably, the  $1/F_{DES}^*$  maps differ significantly from what already obtained in diesel-like conditions, with much larger areas of the spray plume treated as URANS by the seamless switching mechanism.

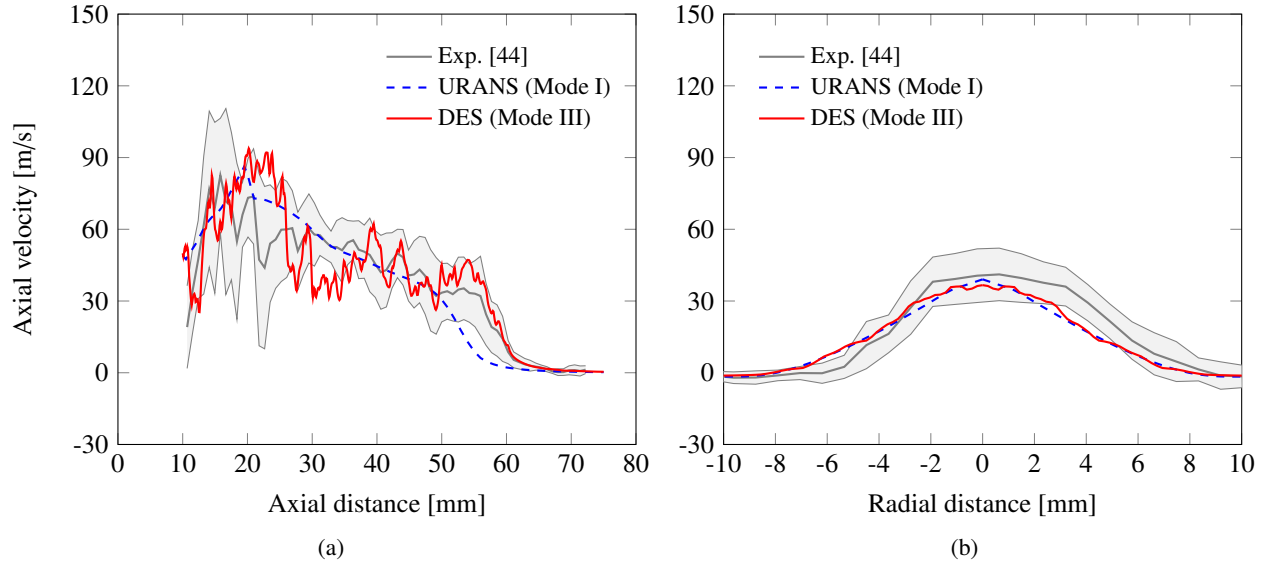


FIGURE 5: Instantaneous a) centerline and b) radial (at 45 mm from the injector) velocity profiles, taken at 1.6 ms after SOI. Results are compared against the experimental data produced at the IFPEN and made available at [46]; the filled area corresponds to the experimental standard deviation.

TABLE 4: “Spray G” nozzle characteristics and operating conditions.

Fuel type	iso-octane ( $C_8H_{18}$ )
Ambient composition (by volume)	0% $O_2$ 6.52% $CO_2$ 3.77% $H_2O$ 89.71% $N_2$
Ambient gas temperature	573 K
Ambient gas pressure	600 kPa
Ambient gas density	3.5 kg/m <sup>3</sup>
Injection duration	0.78 ms
Injection mass	10.4 mg
Injection pressure	20 MPa
Injection temperature	363 K
Nozzle	8-hole
Injector hole diameter	165 $\mu$ m

## CONCLUSIONS

Based on an up-to-date literature survey and on our more recent findings on the proposed topic, we can come to the following conclusions:

- the usage of hybrid URANS/LES turbulence models for fuel spray modeling in engines is, to date, still very uncommon;
- the previous point does not allow, by itself, to formulate strong arguments in favor of or against to the application of such class of models: according to the authors’ opinion, this lack of confidence in hybrids might be due to



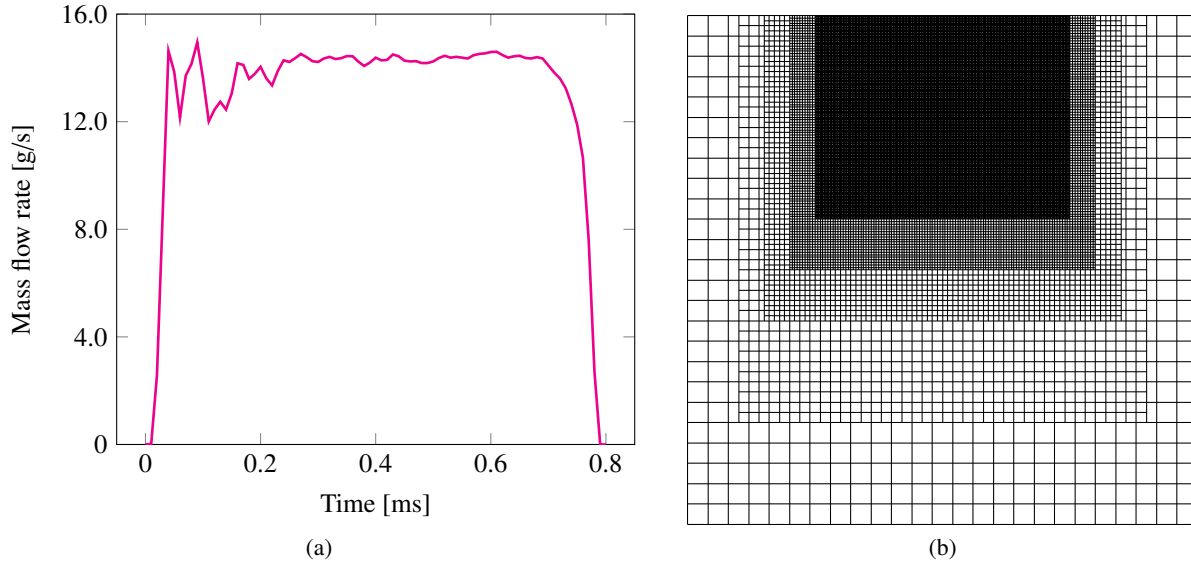


FIGURE 6: a) ROI profile and b) axial section of the mesh adopted for the “Spray G” simulation; the mesh has a minimum cell size of 0.25 mm.

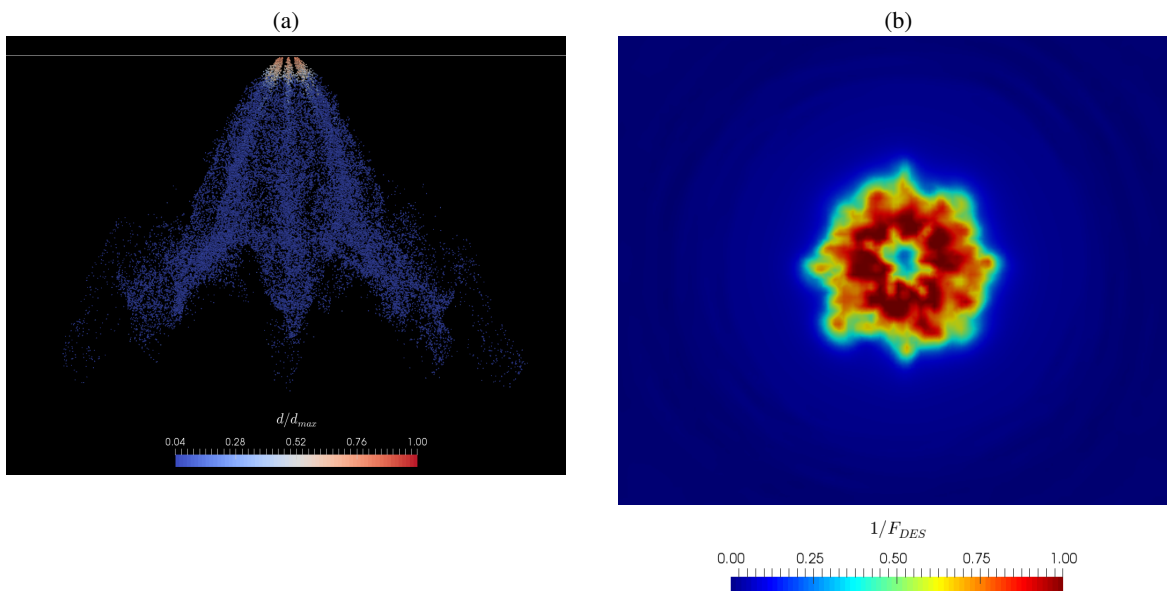


FIGURE 7: a) Spray pattern and b) orthogonal section of the  $1/F_{DES}^*$  function distribution at 10 mm from the injector; both pictures are taken at  $t = 0.3$  ms after SOI.

several factors, the most prominent being the difficulty in foreseeing their actual behavior in the extremely complex, time-varying domains that are typical of engine-related flows;

- from our latest results it seems that, in well-established diesel-like injection conditions (high injection pressure and speed, no cavitation, rapid breakup and vaporization), a standard *seamless* DES dynamic switching mechanism is unable to maintain an URANS-like turbulent viscosity formulation at moderate grid refinement levels, thus essentially acting like a (relatively) coarse LES solution;
- a significantly different behavior emerges in preliminary GDI-like calculations, although the actual reasons have

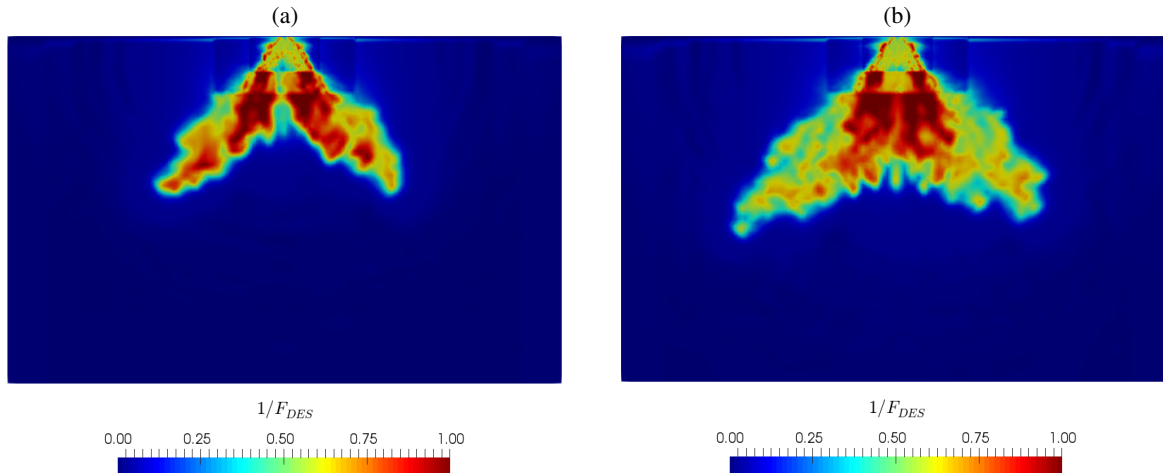


FIGURE 8: Section of the  $1/F_{DES}^*$  function across two spray plumes, taken at a)  $t = 0.4$  ms and b)  $t = 0.6$  ms after SOI.

yet to be fully assessed.

As a follow-up to the conclusions, future investigations should be devoted to: i) a more in-depth analysis of the standard *seamless* DES switching mechanism in a large variety of GDI injection conditions as well as in less canonical diesel-like conditions; ii) the introduction and (eventual) modification of alternative switching mechanism and/or hybrid modeling principles.

## ACKNOWLEDGMENTS

The authors would like to thank Prof. Federico Piscaglia for reviewing the spray breakup libraries developed in the OpenFOAM environment, as well as for fruitful discussion on hybrid turbulence modeling in engines.

## REFERENCES

- [1] [https://ec.europa.eu/growth/sectors/automotive/environment-protection/emissions\\_en](https://ec.europa.eu/growth/sectors/automotive/environment-protection/emissions_en).
- [2] J. M. Garcia-Oliver, J. M. Pastor, A. Pandal, N. Trask, E. Baldwin, and D. P. Schmidt, *Atomization and Sprays* **23**, 71–95 (2013).
- [3] F. J. Salvador, J. Gimeno, J. M. Pastor, and P. Martí-Aldaraví, *International Journal of Multiphase Flow* **65**, 108–116 (2014).
- [4] R. Marcer, P. Le Cottier, H. Chaves, B. Argueyrolles, C. Habchi, and B. Barbeau, *SAE Technical Paper 2000-01-2932* (2000), <https://doi.org/10.4271/2000-01-2932>.
- [5] E. de Villiers, A. Gosman, and H. Weller, *SAE Technical Paper 2004-01-0100* (2004), <https://doi.org/10.4271/2004-01-0100>.
- [6] B. Befrui and M. D’Onofrio, *SAE Technical Paper 2014-01-1125* (2014), <https://doi.org/10.4271/2014-01-1125>.
- [7] M. A. Shost, M.-C. Lai, B. Befrui, P. Spiekermann, and D. L. Varble, *SAE Technical Paper 2014-01-1434* (2014), <https://doi.org/10.4271/2014-01-1434>.
- [8] B. Befrui, M. D’Onofrio, L. E. Markle, and P. Spiekermann, *SAE Int. J. Fuels Lubr.* **8**, 179–189 (2015).
- [9] F. Giussani, A. Montorfano, F. Piscaglia, A. Onorati, J. Hélie, and S. M. Aithal, *Energy Procedia* **101**, 574–581 (2016).
- [10] W. Edelbauer, *Computers & Fluids* **144**, 19–33 (2017).
- [11] C. J. Rutland, *International Journal of Engine Research* **12**, 421–451 (2011).

- [12] S. Fontanesi, A. D'Adamo, and C. J. Rutland, *International Journal of Engine Research* **16**, 403–418 (2015).
- [13] K. Truffin, C. Angelberger, S. Richard, and C. Pera, *Combustion and Flame* **162**, 4371–4390 (2015).
- [14] N. Bharadwaj, C. J. Rutland, and S. Chang, *International Journal of Engine Research* **10**, 97–119 (2009).
- [15] V. Vuorinen, H. Hillamo, O. Kaario, M. Nuutinen, M. Larmi, and L. Fuchs, *Flow, Turbulence and Combustion* **86**, 533–561 (2011).
- [16] A. Wehrfritz, V. Vuorinen, O. Kaario, and M. Larmi, *Atomization and Sprays* **23**, 419–442 (2013).
- [17] M. Jangi, R. Solsjo, B. Johansson, and X.-S. Bai, *International Journal of Heat and Fluid Flow* **53**, 68 – 80 (2015).
- [18] C.-W. Tsang, C.-W. Kuo, M. Trujillo, and C. Rutland, *International Journal of Engine Research in press* (2018), <https://doi.org/10.1177/1468087418772219>.
- [19] C. Hasse, V. Sohm, and B. Durst, *International Journal of Heat and Fluid Flow* **30**, 32–43 (2009).
- [20] C. Hasse, V. Sohm, and B. Durst, *Computers & Fluids* **39**, 25–48 (2010).
- [21] C. Hasse, *International Journal of Engine Research* **17**, 44–62 (2016).
- [22] S. Buhl, F. Hartmann, and C. Hasse, *Oil & Gas Science and Technology - Rev. IFP* **71** (2016), <https://doi.org/10.2516/ogst/2015021>.
- [23] S. Buhl, F. Dietzsch, C. Buhl, and C. Hasse, *Computers & Fluids* **156**, 66–80 (2017).
- [24] S. Buhl, D. Hain, F. Hartmann, and C. Hasse, *International Journal of Engine Research* **19**, 282–292 (2018).
- [25] F. Piscaglia, A. Montorfano, and A. Onorati, *SAE Int. J. Engines* **8**, 426–436 (2015).
- [26] Y. Wu, A. Montorfano, F. Piscaglia, and A. Onorati, *Flow Turbulence Combust* **100**, 797–827 (2018).
- [27] V. K. Krastev, G. Bella, and G. Campitelli, *SAE Technical Paper 2015-24-2414*. (2015), <https://doi.org/10.4271/2015-24-2414>.
- [28] V. K. Krastev and G. Bella, *SAE Int. J. Engines* **9**, 1425–1436 (2016).
- [29] V. K. Krastev, L. Silvestri, G. Falcucci, and G. Bella, *SAE Technical Paper 2017-24-0030*. (2017), <https://doi.org/10.4271/2017-24-0030>.
- [30] V. K. Krastev, L. Silvestri, and G. Falcucci, *Energies* **10**, p. 2116 (2017).
- [31] V. K. Krastev, L. Silvestri, and G. Bella, *SAE Int. J. Engines* **11**, 669–686 (2018).
- [32] V. K. Krastev, G. Di Ilio, G. Falcucci, and G. Bella, *Energy Procedia* **148**, 1098–1104 (2018).
- [33] V. K. Krastev, A. d'Adamo, F. Berni, and S. Fontanesi, *International Journal of Engine Research in press* (2019), <https://doi.org/10.1177/1468087419851905>.
- [34] O. T. Kaario, V. Vuorinen, L. Zhu, M. Larmi, and R. Liu, *Energy* **120**, 827–841 (2017).
- [35] G. Di Ilio, V. K. Krastev, F. Piscaglia, and G. Bella, *SAE Technical Paper 2019-01-0270* (2019), <https://doi.org/10.4271/2019-01-0270>.
- [36] G. Di Ilio, V. K. Krastev, and G. Falcucci, *Energies* **12**, p. 2699 (2019).
- [37] G. Di Ilio, V. K. Krastev, and G. Bella, *SAE Technical Paper 2019-24-0127*. (2019), <https://doi.org/10.4271/2019-24-0127>.
- [38] G. Kalitzin, A. R. B. Gould, and J. J. Benton, *AIAA Paper 96-0327* (1996), 10.2514/6.1996-327.
- [39] G. Bella and V. K. Krastev, in *ASME-JSME-KSME 2011 Joint Fluids Engineering Conference: Volume 1, Symposia Parts A, B, C, and D* (ASME, 2011), pp. 871–883.
- [40] V. K. Krastev and G. Bella, *SAE Technical Paper 2011-24-0163* (2011), <https://doi.org/10.4271/2011-24-0163>.
- [41] P. A. Durbin, *International Journal of Heat and Fluid Flow* **17**, 89–90 (1996).
- [42] P. A. Durbin, *Fluid Dynamics Research* **41**, p. 012203 (2009).
- [43] A. Travin, M. L. Shur, M. Strelets, and P. R. Spalart, in *Advances in LES of Complex Flows*, edited by R. Friedrich and W. Rodi (Kluwer Academic Publishers, Netherlands, 2002), pp. 239–254.
- [44] P. R. Spalart, *Annu. Rev. Fluid Mech.* **41**, 181–202 (2009).
- [45] P. Sagaut, S. Deck, and M. Terracol, *Multiscale and multiresolution approaches in turbulence – LES, DES and Hybrid RANS/LES Methods: Applications and Guidelines* (Imperial College Press, 2013).
- [46] <https://ecn.sandia.gov/>.
- [47] <https://cfd.direct/openfoam/user-guide/>.
- [48] <https://www.cmt.upv.es/ECN03.aspx>.